

Supplement of *Clim. Past*, 16, 2547–2571, 2020  
<https://doi.org/10.5194/cp-16-2547-2020-supplement>  
© Author(s) 2020. This work is distributed under  
the Creative Commons Attribution 4.0 License.



*Supplement of*

## **Plateaus and jumps in the atmospheric radiocarbon record – potential origin and value as global age markers for glacial-to-deglacial paleoceanography, a synthesis**

**Michael Sarnthein et al.**

*Correspondence to:* Michael Sarnthein ([michael.sarnthein@ifg.uni-kiel.de](mailto:michael.sarnthein@ifg.uni-kiel.de))

The copyright of individual parts of the supplement might differ from the CC BY 4.0 License.

1 *SUPPLEMENTARY TEXT. Uncertainties of age control*

2

3 Rough estimates of uncertainty and aspects of analytical quality were published by  
4 Sarnthein et al. (2007, 2015). We now focus on uncertainties tied to the calendar age  
5 definition for each  $^{14}\text{C}$  plateau boundary both in the Suigetsu atmospheric and the  
6 various marine sediment records (Table 1). To recap, an age/sediment section is  
7 formally defined as containing a ' $^{14}\text{C}$  plateau', when  $^{14}\text{C}$  ages show almost constant  
8 values with an overall gradient of  $<0.3$  to  $<0.5$   $^{14}\text{C}$  yr per cal. yr (based on visual  
9 description and/or statistical estimates by means of the 1st derivative of all  
10 downcore changes in the  $^{14}\text{C}$  age – calendar age relationship; Sarnthein et al., 2015)  
11 and a variance of less than  $\pm 100$  to  $\pm 300$   $^{14}\text{C}$  yr, and up to 500  $^{14}\text{C}$  yr prior to 25 cal. ka.  
12 Here  $^{14}\text{C}$  ages form a plateau-shaped scatter band with up to 10% outliers, that extends  
13 over more than 300 cal. yr in the Suigetsu record and/or equivalent sections of marine  
14 sediment depth (following rules defined by Sarnthein et al., 2007).

15

16 On visual inspection a plateau boundary is assigned to the break point between the low  
17 to zero or reversed slope of a  $^{14}\text{C}$  plateau and the normally high regression slope of the  
18  $^{14}\text{C}$  concentration jump that separates two consecutive plateaus (Figs. 1 and S1). More  
19 precisely, a boundary marks the point, where the  $^{14}\text{C}$  curve exceeds the scatter band of  
20 the plateau either crossing the upper or lower envelope line. Thus, the boundary is  
21 chosen about halfway between the last  $^{14}\text{C}$  age within a plateau band and the next  
22 following age outside the scatter band (Figs. 1 and 2). On the U/Th-based model age  
23 scale (Bronk Ramsey et al., 2012) most  $^{14}\text{C}$  dates of the Lake Suigetsu section are  
24 spaced at intervals of  $<10$ – $60$  yr from 10 to 15 cal. ka and  $20$ – $140$  yr between 15 and 29  
25 cal. ka (Fig. 1). Thus the uncertainty of a plateau boundary age assigned halfway

26 between two  $^{14}\text{C}$  ages nearby inside and outside a plateau's scatter band would, on  
27 average, amount to  $\pm 10$ – $\pm 70$  cal. yr.

28

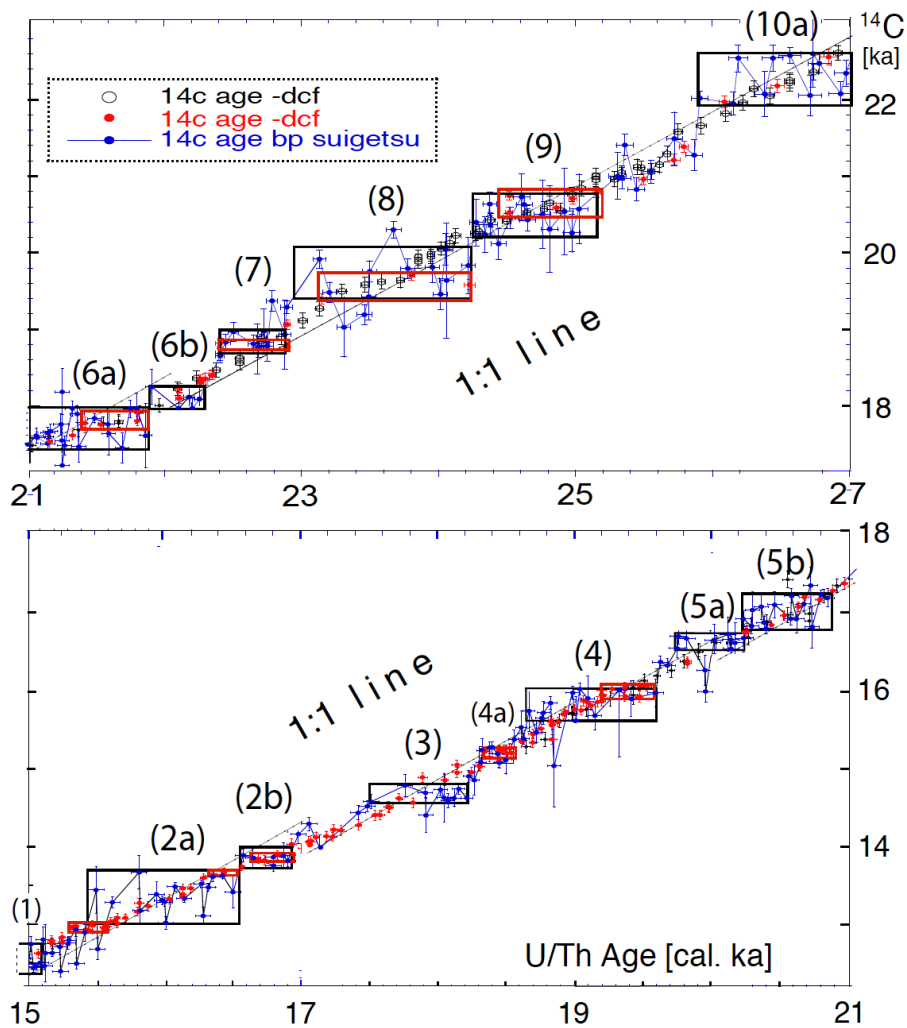
29 In principle, the calendar age uncertainties of marine  $^{14}\text{C}$  plateau boundaries are treated  
30 likewise: After being tuned to those in the Suigetsu  $^{14}\text{C}$  record, the uncertainties are  
31 deduced for the position of all plateaus of a suite within the uncertainty envelope of the  
32 U/Th model-based age calibration. Hence the estimates of total age uncertainty present  
33 the propagated error of the calibrated age of a Suigetsu plateau boundary plus that of  
34 the pertinent plateau in the marine record, where variable depth spacing of  $^{14}\text{C}$  ages is  
35 converted into average time spans.

36

### 37 SUPPLEMENTARY FIGURES

38

39 – Fig. S1. Individual atmospheric  $^{14}\text{C}$  ages and error bars of Lake Suigetsu plant  
40 macrofossils vs. U/Th-based model age of 15–21 (bottom) and 21–27 (top) cal. ka (blue  
41 dots; Bronk Ramsey et al., 2012).  $^{14}\text{C}$  plateaus longer than 250 yr are outlined by a  
42 suite of labeled horizontal boxes that envelop scatter bands of largely constant  $^{14}\text{C}$   
43 ages. Red dots and black circles in Fig. 1a display  $^{14}\text{C}$  ages of Hulu stalagmites. Similar  
44 to  $^{14}\text{C}$  ages of Suigetsu also those of Hulu Cave reveal a suite of  $^{14}\text{C}$  plateaus (red  
45 boxes) tentatively assigned in this figure, plateaus that are shorter than Suigetsu-based  
46 plateaus and occupy slightly different age ranges. The 1:1 line reflects gradient of one  
47  $^{14}\text{C}$  yr / cal. yr.



48

49

50 – Fig. S2. Centennial-to-millennial-scale temporal and spatial variations in planktic (pla.)  
 51 reservoir (res.) and (raw = uncorrected) apparent (app.) benthic  $^{14}\text{C}$  ventilation (vent.)  
 52 ages recorded at 18/20 key sites in the Atlantic (S2a, b, e), Pacific (S2c, d), and Indian  
 53 (S2e). Site locations are given in Fig. 7. Stratigraphic units are marked on top of each  
 54 diagram: Younger Dryas (YD), Bølling-Allerød (B/A) Heinrich Stadial 1 (HS-1), Last  
 55 Glacial Maximum (LGM), and Heinrich Stadial 2 (HS-2).

56 *Origin and various features characteristic of  $^{14}\text{C}$  records:* About 50% of all planktic and  
 57 ('raw') benthic  $^{14}\text{C}$  records were already published in Sarnthein et al. (2015). However,  
 58 the cal. age of all records originally based on microscopy-based varve counts was now  
 59 converted into U/Th-based model ages (Bronk-Ramsey et al., 2012). Planktic  $^{14}\text{C}$

60 reservoir ages of Core GIK23074 are now supplemented by benthic ventilation ages.  
61 Planktic  $^{14}\text{C}$  reservoir ages of SHAK06-5K are detailed in Ausin et al. (2019 and under  
62 review). Benthic ventilation ages plotted for SHAK06-5K are matched from neighbor  
63 core MD99-2334K (Skinner et al., 2014) the stratigraphy and  $^{14}\text{C}$  reservoir ages of  
64 which are closely correlated by means of narrow-spaced suites of  $^{14}\text{C}$  ages. To show an  
65 example, 'raw' benthic ventilation ages in Core MD08-3180 are recalculated into 'actual'  
66 ventilation ages (Balmer and Sarnthein, 2018) that incorporate past changes in  
67 atmospheric  $^{14}\text{C}$  concentration between the time of deep-water formation and the local  
68 growth of benthic foraminifers. South Atlantic  $^{14}\text{C}$  records GeoB3910, GeoB1711-4, and  
69 KNR-159-5-36 (data slightly supplemented) are from Balmer et al. (2016), now  
70 however, with cal. ages converted into U/Th based model ages. The same applies to  
71 MD07-3076, where the continuous planktic and benthic  $^{14}\text{C}$  records are from Skinner et  
72 al. (2010), corroborated by three blue bars reflecting the extent of planktic  $^{14}\text{C}$  plateaus  
73 tuned to atmospheric plateaus no. 1, 2b, and 4. South Pacific  $^{14}\text{C}$  records PS75-104,  
74 SO213-76, MD07-3088, and PS97-137-1 are from Küssner et al. (2018 and under  
75 review; data stored at PANGAEA). Planktic and benthic  $^{14}\text{C}$  records of neighbor cores  
76 GIK17940 and SO50-37, PS75-104 and SO213-84, and ODP893A and MD02-2503  
77 each are plotted on joint graphs, paired records that are obtained from small-scale sea  
78 regions with a common level of planktic  $^{14}\text{C}$  reservoir age. Benthic  $^{14}\text{C}$  ages of SO50-37  
79 and SO213-84 are from Ronge et al. (2016), those of MD07-3088 from Siani et al.  
80 (2013).

Fig. S2a. NORTH ATLANTIC AND NORDIC SEA SITES

WEST and CENTER —

— EAST

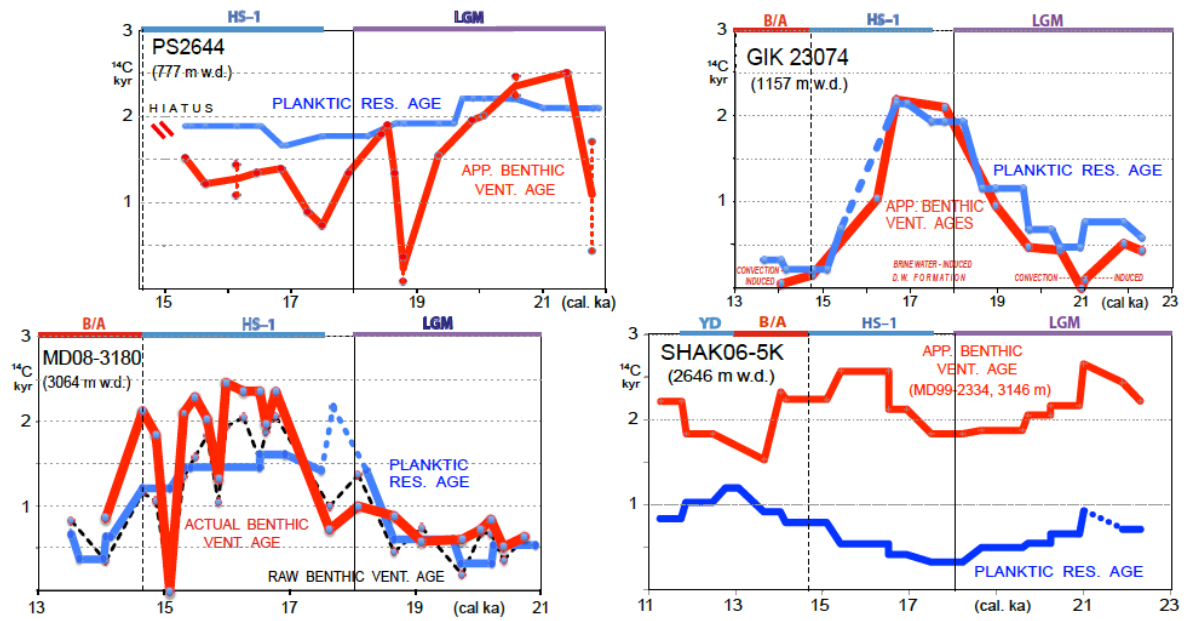


Fig. S2b. SOUTH ATLANTIC SITES

WEST —

— CENTER and EAST

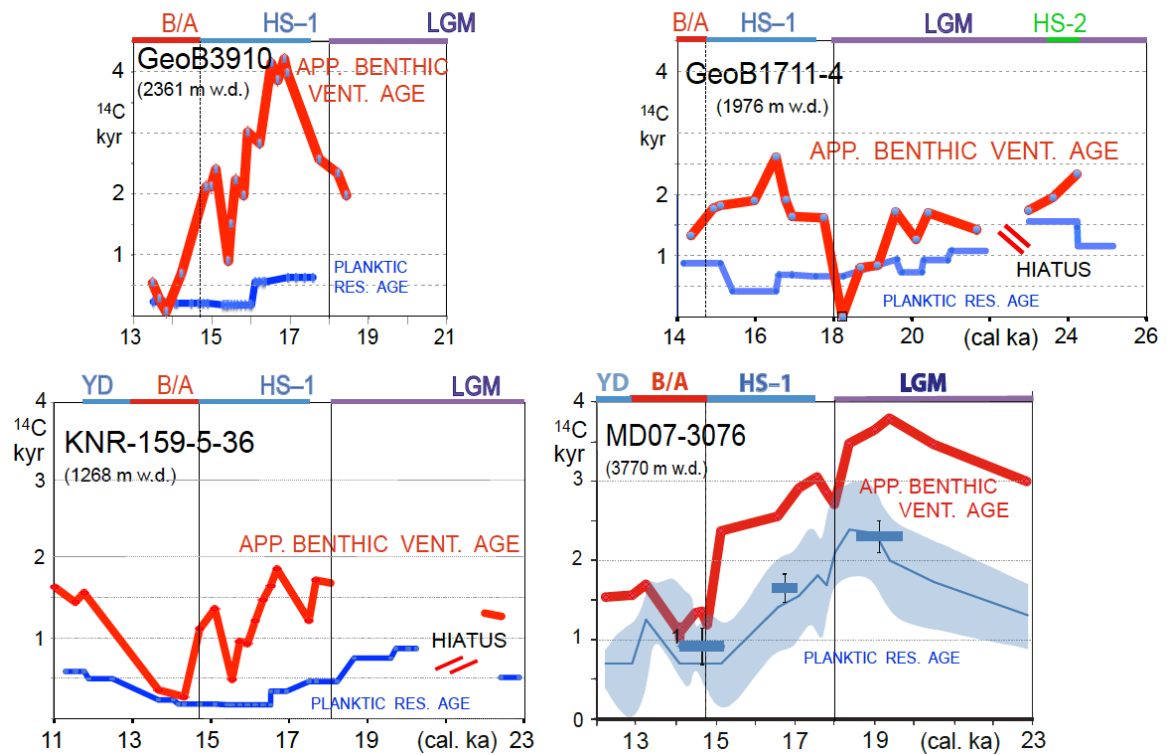


Fig. S2c. SOUTH PACIFIC SITES

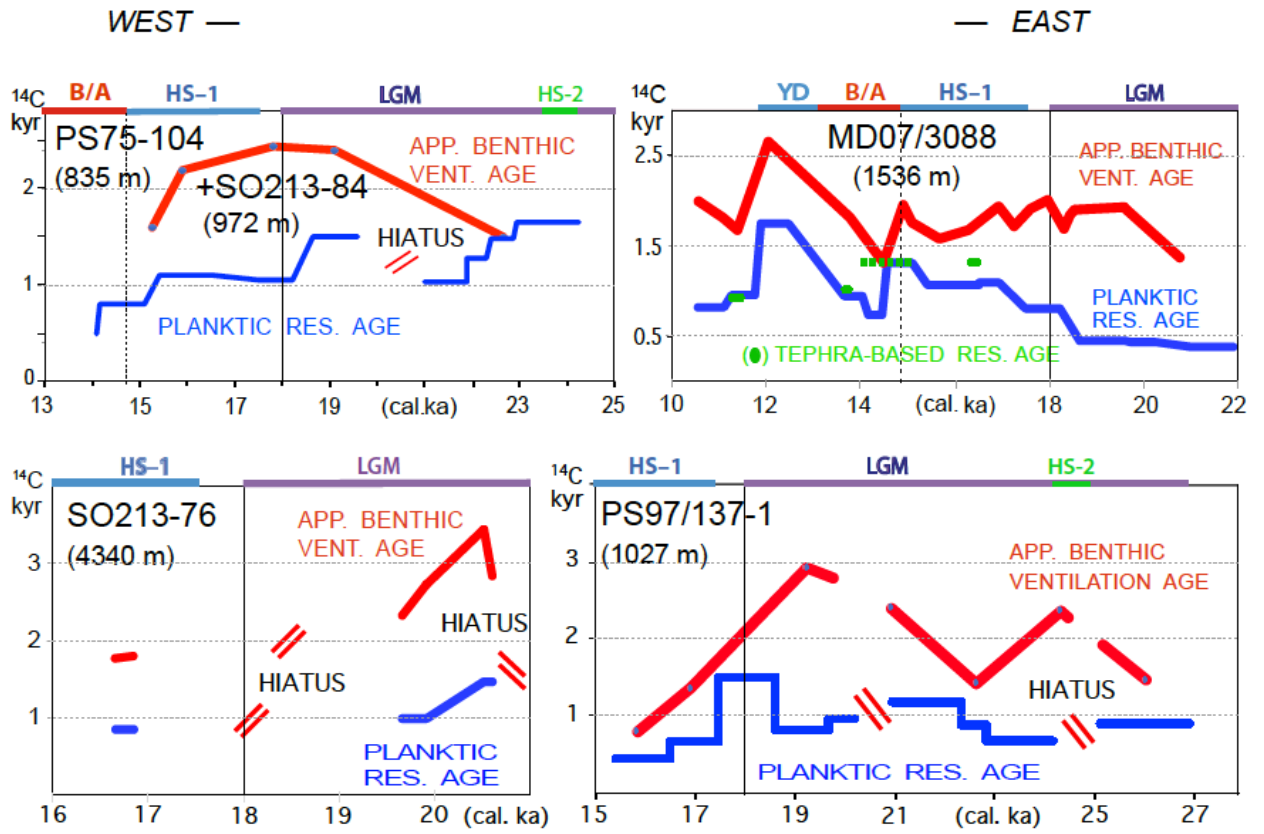


Fig. S2d. NORTH PACIFIC SITES

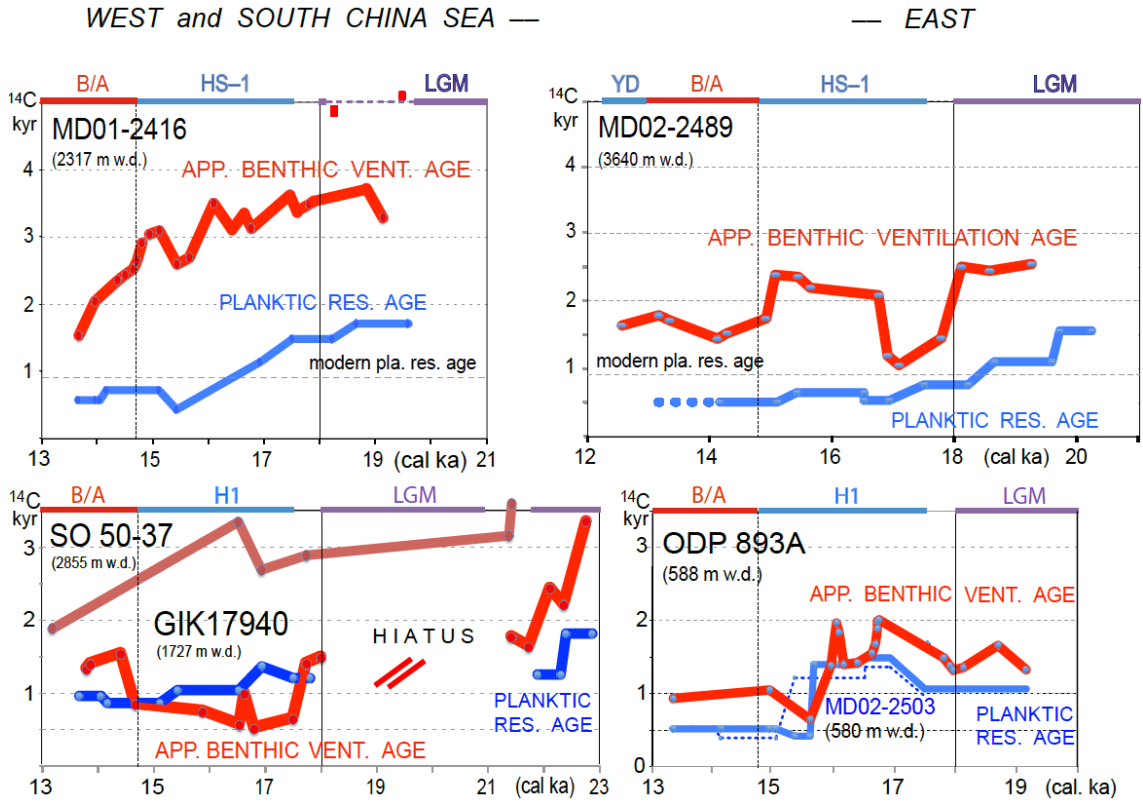
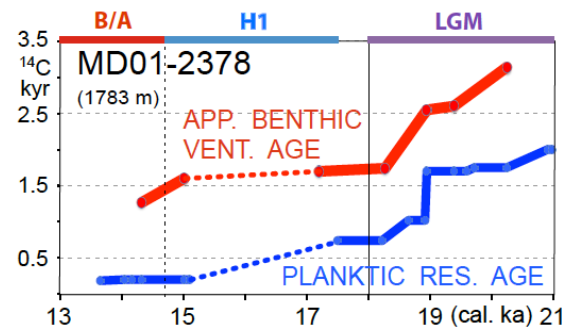
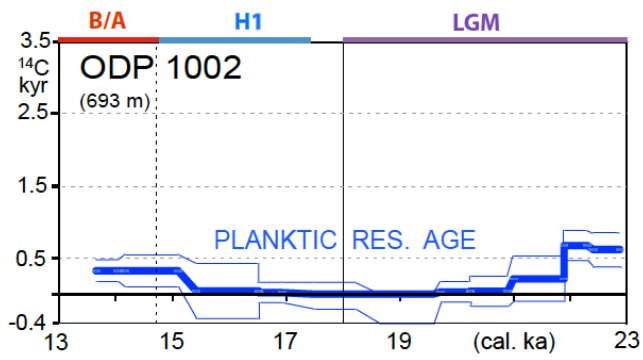


Fig. S2e. SITES in the EQUATORIAL OCEAN

CARIACO BASIN —

— SOUTHERN TIMOR SEA



88

89

90